IL NUOVO CIMENTO Vol. 24 C, N. 2 Marzo-Aprile 2001

Electromagnetic inversion for subsurface applications under the Distorted Born Approximation

R. Pierri, G. Leone, F. Soldovieri(*) and R. Persico

Dipartimento di Ingegneria dell'Informazione, Seconda Università di Napoli
Via Roma 29, I-81031 Aversa, Italy

(ricevuto il 29 Novembre 1999; approvato il 31 Luglio 2000)

Summary. — The problem of reconstructing dielectric permittivity of a buried object from the knowledge of the scattered field is considered for a two-dimensional rectangular geometry at a fixed frequency. The linearization of the mathematical relationship between the dielectric permittivity function and the scattered field about a constant reference profile function and the approximation of actual internal field with the unperturbed field leads to the so-called Distorted Born Approximation. To analyze the limitations and capabilities of the linear inversion algorithms, we investigate the class of the retrievable profiles. This analysis makes it possible to point out that a very reduced number of independent data is available, so requiring to employ regularization techniques in order to perform in a reliable and stable way the linear inversions. In this paper we present a general algorithm consisting in a regularized Singular Value Decomposition of the matrix resulting from a discretization of the problem. Finally, numerical results of linear inversions are given.

PACS 42.30.Wb – Image reconstruction; tomography.
PACS 41.20.Jb – Electromagnetic wave propagation; radiowave propagation.
PACS 42.25.Fx – Diffraction and scattering.

1. – Introduction

The problem of determining location and internal properties of buried objects from scattered field data is of interest for many applications, ranging from archaeological prospecting to the detection of utilities and civil engineering. The most common way of operation of the appropriate radar system encompasses the interpretation of time domain traces to locate discontinuities in the underground medium. However, this procedure is mainly founded on the ability and the experience to interpret the raw data while it would be more interesting to directly have at one's disposal tomographic views of subsurface.

(*) Currently Researcher at Istituto per il Rilevamento Elettromagnetico dell'ambiente IREA-CNR

This goal can be accomplished only by investigating in detail the mathematical relationship connecting the electrical properties of both the buried objects and the embedding medium to the electromagnetic scattered field. This is necessary for facing the inverse problem of reconstructing the unknown dielectric profile function.

As is well known, this is a nonlinear and ill-posed problem [1]. A possible way for solving it entails the linearization of the mathematical relationship about a chosen reference profile function and the approximation of actual internal field with the unperturbed field, that is the field in the absence of the scattering objects, giving arise to the so-called Distorted Born Approximation (DBA) [2].

In the following we stay within this approximation and refer to a geometry consisting of two homogeneous half spaces, one of which is the free space. In addition, we consider objects which are invariant along one coordinate parallel to the interface and with infinite extent along this direction. When we assume filamentary sources of infinite length parallel to the objects, the problem at hand has a full two-dimensional geometry. We suppose to fix the working frequency, that the source can move in the free space along a line orthogonal to the direction of invariance of the objects (multiview excitation) and that the scattered field is probed along the same line in different locations (multistatic configuration). As will be shown below, the geometry of the problem naturally lends itself to discussions within the Fourier-transformed spectral domain.

The same observation geometry, although with plane-wave excitation, have been considered also in [3], where the observation of spectral coverage allows to sketch some limitations about the profile functions to be retrieved. In particular it is recognized that "reflection" mode configuration implies some "hole" in the lower part of the spectral domain and suggestions for increasing the extent of the spectral coverage are given. However, the inversion algorithm does not cope with the presence of a lossy half-space and, above all, it does not account for ill-conditioning of the linear operator to be inverted. The same limitations are also in [4] where the lack of data is illusively counteracted by an extrapolation procedure requiring, however, *a priori* knowledge about the magnitude of data to be reconstructed. Other works [5-7], relying on the monostatic measurement configuration, require multifrequency data and provide inversion algorithms, but do not discuss about the role of additional information with respect to the unknowns to be searched for.

The aim of the paper is, rather than to establish a new inversion procedure, to discuss some limitations of the inversion procedure based on the DBA linear model. This is accomplished by analyzing the relevant linear operator in the DBA approximation thanks to the Singular Value Decomposition (SVD) tool [8, 9].

A similar analysis has been already performed within the context of the Born approximation for the so-called weak scatterers and has led to show that it entails limitations on the spatial variability of dielectric profiles that can be reconstructed [10]. When dealing with the DBA for a homogeneous cylinder [11] the role of the reference permittivity has been put in evidence in determining the class of the retrievable functions.

Some important conclusions can be drawn in the lossless case and most discussion applies also for a lossy half-space. The key point to be observed is that, when the observation line is located sufficiently far (at more than a wavelength) from the interface, the scattered field can be represented within a finite-dimensional space whose dimension is not strictly dependent on the noise level. This entails that only a finite amount of independent data can be obtained from measurements. Accordingly, it is hopeless to search for a number of unknowns larger than the number of independent data. In other words, the class of retrievable unknown functions is within a finite-dimensional space

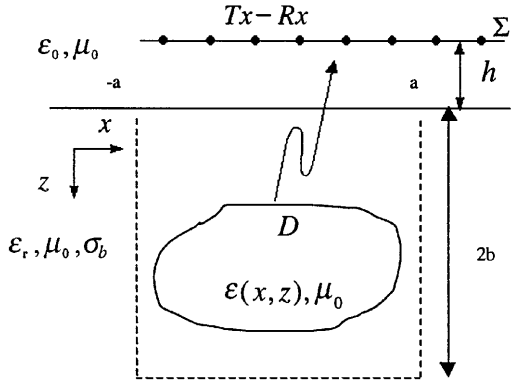

Fig. 1. – Geometry of the problem.

spanned by basis functions which, as will be inferred in the following, have some peculiar spatial variability properties.

The very reduced number of available independent data makes it necessary to employ regularization techniques in order to invert the linear relationship in a reliable and stable way. Moreover, while in the lossless case fast-inversion algorithms based on the Fourier transform [3] can be devised, in the lossy case this is not possible. So we propose a reconstruction algorithm based on the regularized inversion of the linear integral equation relevant to the DBA model where the unknown is searched within a prescribed finite-dimensional space and a point matching technique enforces the equation in an arbitrary set of points. This allows to account for the truncation of the observation domain and to consider possible constraints on the positions of the receiver.

In the following section the formulation of the problem within the DBA is given and the relevant linear operators are introduced. In sect. **3** the case of a lossless half-space is dealt with so to provide the main limitations of the linear model by examining the spectral domain; then the case of a lossy half-space is also dealt with. The solution algorithm is presented in sect. **4** where also numerical examples are given. Conclusions follow in sect. **5**.

2. – The linear model of the scattered field

The geometry of the problem is depicted in fig. 1. The unknown of the problem to be reconstructed is the relative, possibly complex, permittivity ε function within a rectangular domain D of interest, which is embedded in a homogeneous half-space whose relative dielectric permittivity and conductivity are ε_{r} and σ_{b}, respectively. The domain D is assumed to be rectangular with $|x| \leq a$ and $0 \leq z \leq 2b$; this means that a rough *a priori* information about the position of the scattering object is available. The absolute dielectric permittivity of the upper half-space equals that of the free space ε_0, and the magnetic permeability is everywhere equal that of to the free space μ_0. The source of the incident field is a filamentary y-oriented either electric (the TM polarization, the scalar case) or magnetic (the TE polarization, the vector case) current distribution, at a fixed pulsation ω (the time dependence $\exp[j\omega t]$ is assumed) and located at the abscissa x_{s}. The electric field scattered by the buried object is measured at the abscissa x, where x_{s} and x vary along the straight line Σ, at quote $z = h \leq 0$.

In the following let us denote by $\mathbf{E}_{\text{inc}}$ the unperturbed incident field in the lower half-space, (*i.e.* the electrical field for $z > 0$ when the scattering object is absent) and by $\mathbf{E}_{\text{s}}$ the electrical field scattered by the buried object. Moreover, $k_0 = \omega\sqrt{\varepsilon_0\mu_0}$ and $k_{\text{s}} = k_0\sqrt{\varepsilon_{\text{r}} - j\sigma_{\text{b}}/(\omega\varepsilon_0)}$ are the wave numbers in the free space (*i.e.*, in the upper half-space) and in the lower half-space, respectively. The problem is recast in terms of the adimensional contrast function, defined as

$$\chi = \frac{\varepsilon_0\varepsilon(x,z) - \varepsilon_{\text{b}}}{\varepsilon_{\text{b}}}, \tag{1}$$

where ε_{b} is the background permittivity function, defined as ε_0 for $z < 0$ and $\varepsilon_{\text{r}}\varepsilon_0 + \sigma_{\text{b}}/j\omega$ for $z > 0$. By definition of ε_{b}, the contrast function is equal to zero outside the investigation domain D (see fig. 1).

Within the DBA, the contrast and the scattered field on Σ are linked by the following linear relationship:

$$\mathbf{E}_{\text{s}}(x, x_{\text{s}}, h) = k_{\text{s}}^2 \iint_D \underline{\mathbf{G}}_{\text{e}}(x, h, x', z')\mathbf{E}_{\text{inc}}(x', z', x_{\text{s}}, h)\chi(x', z')\,\mathrm{d}z'\,\mathrm{d}x', \quad (x, x_{\text{s}}) \in \Sigma, \tag{2}$$

where $\underline{\mathbf{G}}_{\text{e}}(x, z, x', z')$ is the external dyadic Green's function (*i.e.*evaluated when $z < 0$ and $z' > 0$) of the inhomogeneous background permittivity which, for the 2D geometry of our concern, is known in closed form expressed by a spectral integral [12,13]. Also the incident field can be straightforwardly computed under a plane-wave (spectral) expansion. It is now convenient to introduce the two-dimensional Fourier transform (TDFT) of the scattered field with respect to the source position x_{s} and the receiver location x

$$\hat{\tilde{E}}_{si}(u, u', h) = \int_{-\infty}^{+\infty}\int_{-\infty}^{+\infty} E_{si}(x_{\text{s}}, x, h)\exp[jux_{\text{s}}]\exp[ju'x]\,\mathrm{d}x_{\text{s}}\,\mathrm{d}x, \tag{3}$$

where the subscript i refers to one of the x, y or z Cartesian components.

If we define the following integral transform of the contrast function with respect to the horizontal abscissa x and the depth quota z

$$\tilde{\hat{\chi}}(\eta, \zeta) = \int_{-\infty}^{+\infty}\mathrm{d}z\int_{-\infty}^{+\infty}\mathrm{d}x\,\chi(x, z)\exp[j\eta x]\exp[-j\zeta z], \tag{4}$$

where η is a real variable and ζ is a complex one, a simple proportional relationship connects it to the TDFT of each component of the scattered field for both polarisations.

In particular in the TM polarization, where the only field component is along the y-axis, we obtain (see appendix)

$$\hat{\tilde{E}}_{sy}(u, u') = f_{\text{TM}}(u, u')\exp\big[j\big[w_0(u) + w_0(u')\big]h\big]\tilde{\hat{\chi}}\big(u + u', w_{\text{s}}(u) + w_{\text{s}}(u')\big), \tag{5}$$

where

$$f_{\text{TM}}(u, u') = \frac{jk_{\text{s}}^2\mu_0\omega}{[w_0(u) + w_{\text{s}}(u)][w_0(u') + w_{\text{s}}(u')]} \tag{6}$$

$$w_i(\nu) = \sqrt{k_i^2 - \nu^2}, \quad i = 0, \text{s}. \tag{7}$$

If the source is a magnetic current filamentary distribution (TE polarization), the scattered field has two components E_{sx} and E_{sz}, along the x- and the z-axis, respectively. Also in this case, within the Distorted Born Approximation, it is possible to work out two linear spectral relationships between the components of the TDFT of scattered field and the contrast (the calculations are detailed in appendix) as

$$\hat{\tilde{E}}_{sx}(u,u') = f_{\mathrm{TE}}(u,u')\exp\left[j\left[w_0(u)+w_0(u')\right]h\right]\tilde{\tilde{\chi}}\left(u+u', w_{\mathrm{s}}(u)+w_{\mathrm{s}}(u')\right), \tag{8}$$

$$\hat{\tilde{E}}_{sz}(u,u') = \frac{u'}{w_0(u')} f_{\mathrm{TE}}(u,u')\exp\left[j\left[w_0(u)+w_0(u')\right]h\right]\tilde{\tilde{\chi}}\left(u+u', w_{\mathrm{s}}(u)+w_{\mathrm{s}}(u')\right), \tag{9}$$

where

$$f_{\mathrm{TE}}(u,u') = \frac{j\varepsilon_{\mathrm{r}}}{[\varepsilon_{\mathrm{r}} w_0(u)+w_{\mathrm{s}}(u)][\varepsilon_{\mathrm{r}} w_0(u')+w_{\mathrm{s}}(u')]} w_0(u')[w_{\mathrm{s}}(u)w_{\mathrm{s}}(u')+uu']. \tag{10}$$

From eqs. (5), (8) and (9) it follows that, apart a common exponential factor accounting for the propagation of plane waves in the free space up to the height h, the field components are related to each other by a linear relationship and the only difference between them relies in factors (6) and (10). In spite of the fact that, strictly speaking, their presence affects the operational relationship between the unknown profile and the data, it can be expected that, since both of them are not rapidly varying functions, the fundamental properties of the two linear operators (as far as the number and kind of retrievable profile functions is concerned) are very similar since related to the properties of the common integral transform, that is to the term $\tilde{\tilde{\chi}}(u+u', w_{\mathrm{s}}(u)+w_{\mathrm{s}}(u'))$. In fact, in this circumstance, the transformed components of the contrast, for the same arguments, are weighted in a similar way for the two kinds of polarization as long as the factors f_{TM} and f_{TE} do not contain singularities or different complex exponential terms. Therefore, within the DBA, the spectra of such scattered field components, and consequently also the scattered fields themselves, are not too much different since they share a common behavior with respect to the object contrast function. So, it is to be expected that the relationships between the unknown profile and the scattered field are not linearly independent in the two polarizations. Conversely, results provided by inversion algorithms within the framework of the DBA are expected to be very similar, which means that probing the scattered field under both measurement configurations cannot provide further independent information with respect to the one available by a single component of the scattered field.

Of course when actual scattered field data (that is computed without any model approximation) are considered, the linear inversion can give different results for the two kinds of polarization, because the range of validity of each approximations can be different. The question of determining the polarization for which the linear model has the widest range of validity should be then addressed, but is beyond the purposes of this work.

We will refer our analysis to the scalar case because, for the discussion to follow, the choice of the polarization makes no meaningful difference.

3. – The essential dimension of the scattered field

Let us first rely on the case when both a lossless half-space ($\sigma_{\mathrm{b}} = 0$) and a lossless object ($\sigma = 0$) are considered, since this makes it possible to provide some general

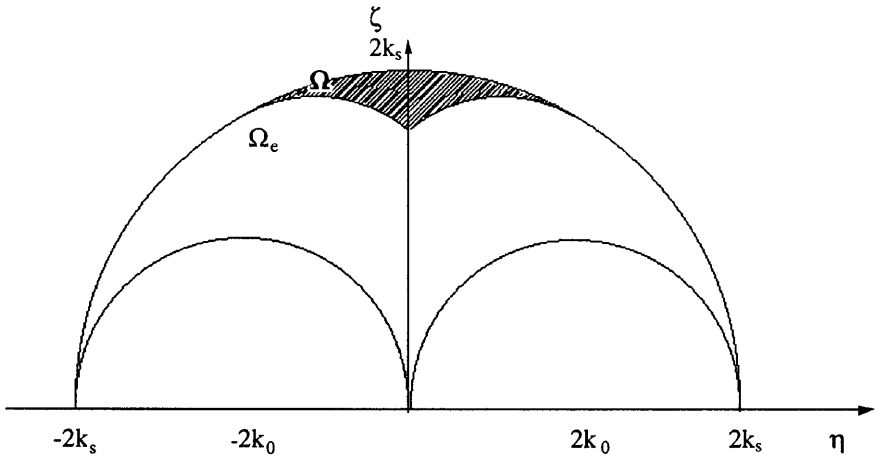

Fig. 2. – Spectral domain covered by the linear model. The horizontal axis refers to the x-spatial variability, the vertical one refers to z-spatial variability. Regions Ω and Ω_e correspond to $h \geq \lambda$ and $h = 0$, respectively.

considerations on the "number" and the features of contrast profiles retrievable.

Then, as long as $|u|, |u'| \leq k_s = \omega\sqrt{\varepsilon_0 \varepsilon_r \mu_0}$, *i.e.* w_s is a real function, on the right-hand side of (4) the TDFT of the contrast function appears, since both independent variables η and ζ are real.

Furthermore, when the w_s functions become imaginary for ($|u|, |u'| > k_s$) if the object is buried at a depth greater than one wavelength, the corresponding evanescent plane waves contribute in a negligible way to the field scattered by the object. Therefore, TDFT of the contrast function turns to be proportional to the TDFT of the scattered field according to the mapping defined as

$$\begin{aligned} \eta &= u + u', \\ \zeta &= w_s(u) + w_s(u'), \end{aligned} \tag{11}$$

and it is possible to obtain information about the TDFT in a finite set Ω_e [3] whose extent depends on frequency and ε_r (fig. 2). The examination of the geometry of Ω_e allows to observe relevant "holes" in the spectral coverage at lower spatial harmonics of the contrast function. Moreover, when the quota h of the observation line is larger than some free space wavelength, the scattered field spectrum becomes meaningful only for pairs (u, u') such as $|u|, |u'| \leq k_0 < k_s$. This is because the exponential factor in (5) provides a strong attenuation of the field spectrum when $|u| > k_0$ and/or $|u'| > k_0$. As a consequence, because of (11) the set of spatial frequencies where the TDFT transform of the contrast is available shrinks from Ω_e to a subset Ω depicted in fig. 2. In fact, the evanescent part of the spectrum radiated in free space has decayed to negligible levels with the result that the corresponding spectral information about the object is lost.

Note that the maximum extent of Ω with respect to the horizontal spatial harmonic is $2k_0$, while with respect to the vertical harmonic variable ζ, this extent amounts to $2k_s - 2\sqrt{k_s^2 - k_0^2} \approx k_0/\sqrt{\varepsilon_r}$, a figure reducing as the relative dielectric permittivity of the half-space increases.

Let us remark that a very similar behavior has been already observed within the DBA for a homogeneous circular cylinder when dealing with radial variations [9]. In fact, also in that circumstance, the dimension of the subspace of the profile functions that can be reconstructed by linear inversion reduces as ε_r increases and it comprises spatially rapidly varying functions with a relevant harmonic content around the spatial pulsation $2k_s$.

The above observation means that the class of the retrievable contrast functions within the DBA is essentially related to the geometrical characteristics of set Ω. Therefore, it is to be expected that it comprises functions with a "low-pass" behavior with respect to the horizontal variations (Ω is located in a low horizontal spatial frequency area) and with a "band-pass" behavior with regard to the vertical variations (Ω is located close to the vertical spatial pulsation $2k_s$) and in any case it is made of a reduced number of independent functions.

Moreover, the fact that either Ω or Ω_e is finite implies that, at any rate, only a finite number of unknowns can be reconstructed. According to results in [14-16], concerning the finite Fourier transform relationship operator, the number of the unknowns to be searched for is related to the product between the measure A of the domain D of the contrast function and the measure of the spectral area where the Fourier transform of the contrast is available, when this product is much larger than one.

Accordingly, if m is the measure of the set where the spectrum of the contrast can be reliably reconstructed, we expect that the number of unknowns that can be retrieved is roughly

$$N = \frac{Am}{4\pi^2}, \tag{12}$$

which becomes, when h is larger than some wavelength and $\varepsilon_r \gg 1$,

$$N \cong \frac{A}{4\lambda^2\sqrt{\varepsilon_r}}, \tag{13}$$

where λ is the free space wavelength. Note that, due to the refraction, this figure reduces as the relative permittivity of the lower half-space increases. For a comparison, it can be noted that the same object embedded in a homogenous background equal to the embedding medium would provide the higher bound $\pi A\varepsilon_r/\lambda^2$.

Moreover for the problem at hand in this paper, concerning a domain of some free space wavelengths extent, the product of the area of domain D with the area of the allowable spectral domain Ω is small. Therefore, some considerations can be inferred by observing the numerically computed SVD of the relevant operator within the DBA approximation. We accomplish this computation by expanding the contrast function according to a finite Fourier series and using a point-matching procedure in the spectral domain (u, u'). A reliable approximation of the SVD is obtained when the increase in the discretization grid does not affect the behavior of the singular values.

Figure 3 depicts the behavior of the singular values for different values of the relative dielectric permittivity of the medium when the extent of the investigation domain is equal to $3\lambda \times 3\lambda$ and the height of the observation domain is $h = \lambda$. First, the decay of the singular values is rather smooth, so preventing the definition of the number of degrees of freedom as the parameters defining the scattered field which are weakly dependent

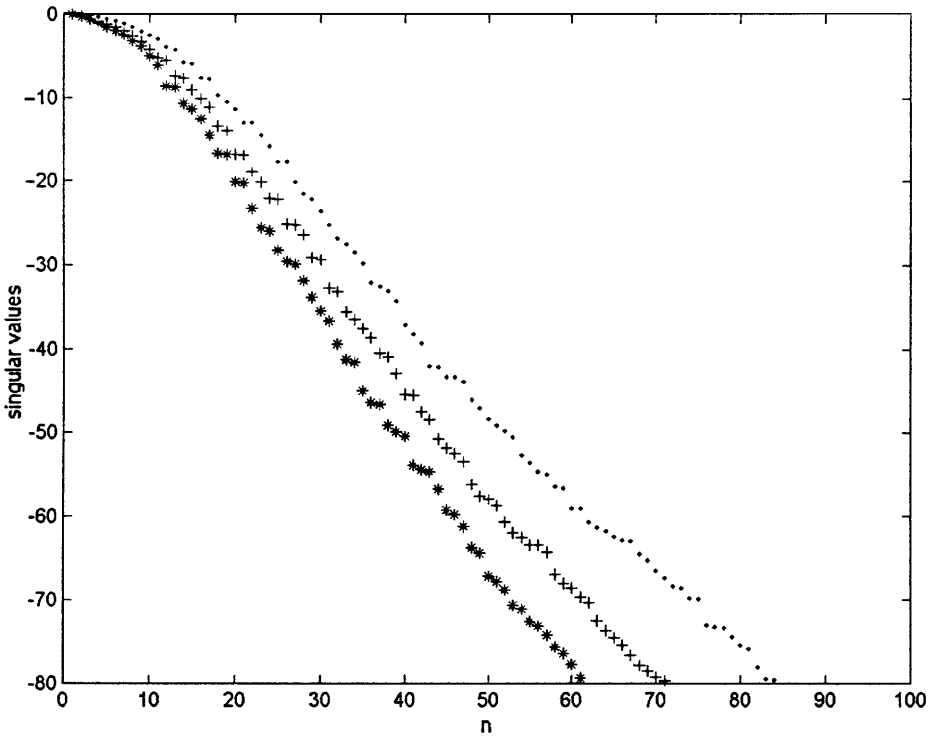

Fig. 3. – Singular values of the relevant linear operator, normalized to the maximum, for $2a = 3\lambda$ and $2b = 3\lambda$ and three values of ε_r ($\bullet$ $\varepsilon_r = 5$; $+\varepsilon_r = 10$; $*$ $\varepsilon_r = 20$).

on the noise level. Second, as expected according to (13), we observe a decrease in the number of the significant singular values as the dielectric permittivity increases.

Figure 4 depicts the behavior of the singular values for a fixed value of the dielectric permittivity corresponding to different extent of the source domain; as expected, the number of significant values increases when the extent of the domain becomes larger.

The harmonic content of the singular functions expanding the contrast has also been observed and the singular functions corresponding to the significant singular values have a relevant harmonic content at low frequencies for spatial variations along the x-axis and at the spatial frequency $2k_s$ for the z-variations.

The general formulation introduced in sect. **2** copes also with the case of a lossy half-space, with the only remark that now the $w_s(\cdot)$ functions, and thus also ζ, are to be meant as complex quantities. Therefore, (11), for real values of u, u', provides a surface in the three-dimensional space $(\eta, \mathrm{Re}(\zeta), \mathrm{Im}(\zeta))$, and so the square domain $|u|, |u'| < \mathrm{Re}(k_s)$ is now mapped into a finite not-planar surface in a three-dimensional space. This implies that, again, the number of independent data is finite, and accordingly only a finite number of unknowns can be reconstructed.

The SVD analysis can be seen as a first step towards the establishment of a proper inversion procedure in order to define the correct (maximum) number of independent parameters of the unknown permittivity function that can be extracted. Since this figure, according to the above discussion, can be very low, the retrievable profile function

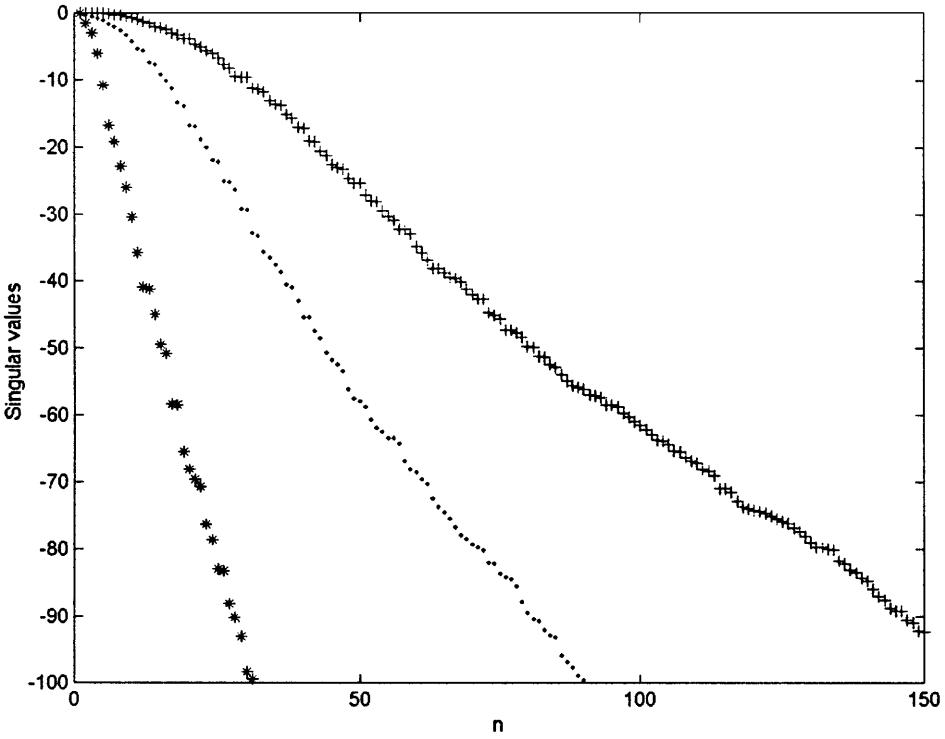

Fig. 4. – Singular values of the relevant linear operator, normalized to the maximum, for $\varepsilon_r = 10$ and square source domains with three different values of side $2a$ ($* \; 2a = \lambda$; $\bullet \; 2a = 3\lambda$; $+ \; 2a = 5\lambda$).

should be well-approximated by a properly chosen set of functions and an exceedingly high number of unknowns (as resulted *e.g.* from the discretization of the unknown into pixellated rectangular pulse functions) should be avoided. Moreover, the presence of unavoidable uncertainties in data requires a careful inversion scheme which would provide a stable reconstructed image and achieve the best spatial resolution.

An increase in the amount of the spectral information (to cover Ω_e) on the buried object could be obtained by locating the sources and the receivers as close as possible to the interface. However, some cautions, due to some practical limitations preventing the coverage of the whole Ω_e, have to be taken into account.

First, due to the non-linearity of the mapping (11), the available spectral information is not "uniformly spread" within Ω_e, but the lower spectral content of the scattered field (corresponding to $u^2 + u'^2 \leq k_s^2$) maps closer to Ω. On the contrary, the contributions around the origin of the spectral plane (ζ, η) are due to faster spatial harmonics of the scattered field.

Second, if we consider a nonideal source, with a radiation pattern in free space different from the one of the isotropic source, we expect that its plane-wave spectrum, that multiplies the plane-wave components of the scattered field, weighs the higher-order spectral contributions of the scattered field at a decreasing extent.

A further limitation is due to the fact that the line Σ cannot be infinitely extended, so that the exact TDFT of the scattered field cannot be evaluated but only a smoothed

version is available due to the convolution of TDFT with the transform of a square pulse function of side equal to the extent of the finite truncated probing domain Σ; this surely restricts the spectral coverage in the plane (η, ζ).

In addition, to obtain data at higher spatial frequencies requires the scattered field to be sampled at an increasing rate, but this can be impractical in many circumstances for the finite physical extent of the sources and receivers. Furthermore, in multistatic configurations, with different antennas for source and receiver, the monostatic datum may not be available.

So, we can conclude that it is not possible, from the scattered field data, to obtain reliably information about the TDFT of the contrast in a set much larger than Ω.

4. – The inversion algorithm and the numerical results

In this section some results of an extensive numerical analysis for TM polarization are presented with the aim to show the effect of various parameters on the reliability and precision of the inversions. We want also to take into account the fact that field data, scattered under arbitrarily located excitation sources, might be collected only at prescribed locations at quota h. Therefore, the solution algorithm should be properly formulated within the spatial domain. On the other side, the considerations of the above section confirm that only a finite number of unknowns can be reconstructed, and suggest to introduce an appropriate finite-dimensional space wherein to search for the unknown permittivity function. In this paper we adopt the choice of separating the vertical form the horizontal variations in the unknown function, so that

$$\chi(x,z) = \sum_{m=1}^{M} \sum_{n=-N}^{N} \chi_{mn} \psi_m(z) \varphi_n(x), \tag{14}$$

where the choice of basis functions expanding the unknown should be performed taking into account any *a priori* information about the solution of problem.

By substitution of (14) into (4) and next into (5), we obtain

$$\hat{\hat{E}}_{sy}(u,u') = f_{\mathrm{TM}}(u,u') \exp\left[j(w_0(u) + w_0(u'))h\right] \sum_{m=1}^{M} \sum_{n=-N}^{N} \chi_{mn} \tilde{\psi}_m(u,u') \hat{\varphi}_n(u,u'), \tag{15}$$

where

$$\begin{aligned} \tilde{\psi}_m(u,u') &= \int_0^{\infty} \psi_m(z') \exp\left[-j\left[w_{\mathrm{s}}(u) + w_{\mathrm{s}}(u')\right]z'\right] \mathrm{d}z', \\ \hat{\varphi}_n(u,u') &= \int_{-\infty}^{\infty} \varphi_n(x') \exp\left[j(u+u')x'\right] \mathrm{d}x'. \end{aligned} \tag{16}$$

By double inverse Fourier transforming (15) we come to the following linear relationship between the unknown coefficients χ_{nm} and the scattered field data:

$$E_{sy}(x_{\mathrm{s}}, x) = \sum_{m=1}^{M} \sum_{n=-N}^{N} \chi_{mn} p_{nm}(x_{\mathrm{s}}, x), \tag{17}$$

where the functions p_{nm} are provided by

$$(18)\qquad p_{nm}(x_{\mathrm{s}},x)=\frac{1}{(2\pi)^2}\int_{-\infty}^{+\infty}\int_{-\infty}^{+\infty} f_{\mathrm{TM}}(u,u')\exp\left[j\big(w_0(u)+w_0(u')\big)h\right]\times \\ \times\,\tilde{\psi}_m(u,u')\hat{\varphi}_n(u,u')\exp\left[-jux_{\mathrm{s}}\right]\exp[-ju'x]\,\mathrm{d}u\,\mathrm{d}u'.$$

A system of linear equations is obtained by imposing that (17) is satisfied in a set of points equal or larger than the number $(2N+1)M$ of the unknowns. In order to provide a stable and reliable inversion of the resulting matrix we have employed the numerical filtering method [17] based on the Singular Values Decomposition algorithm [8], consisting in approximating the solution onto the finite-dimensional space spanned by the left singular functions corresponding to the singular values greater than a prescribed threshold (equal to 1/100 of the maximum singular value in the test-cases to follow), which can be interpreted as a "signal-to-noise ratio".

For the test-cases at hand, we search for the unknown in a finite-dimensional space given by (14) with

$$(19)\qquad \varphi_n(x)=\exp\left[\frac{-jn\pi x}{a}\right]\qquad \psi_m(z)=\mathrm{rect}\left[\frac{(z-z_m)}{\Delta z}\right],$$

where $\Delta z=2b/M$ and $z_m=(m+1/2)\Delta z$ and $\mathrm{rect}(\cdot)$ is a rectangular pulse function of unitary width centered at $z=0$. Therefore, we assume basis functions along the x-axis defined over the entire domain and subsection basis functions along the z-coordinate. The adopted choice of the basis function along the z-axis seems convenient when the additional *a priori* information about the unknown function about the rectangular pulse behavior of the unknown is available, as we will suppose.

In order to show the filtering features of the linear relationship between the scattered field and the contrast function, we assume as data of the problem the DBA of the scattered fields.

First results concern the observation domain at the height $h=\lambda$ and we assume the data in the spectral domain; this is equivalent to consider a spatial domain, wherein the sources radiate and receive, sufficiently large to ensure the decay of the amplitude of scattered field at negligible values. The first result concerns two objects of rectangular section of extent $0.75\,\mathrm{m}\times 1\,\mathrm{m}$ whose centers are located at $(-0.625\,\mathrm{m}, 1.5\,\mathrm{m})$ and $(0.625\,\mathrm{m}, 1\,\mathrm{m})$ respectively, with $\varepsilon=10.1-j0.42$. The domain D has extent $2a=2.5\,\mathrm{m}$ along the x-axis and a depth of $2b=3\,\mathrm{m}$, with the embedding medium having $\sigma_{\mathrm{b}}=7\times 10^{-3}\,(\Omega\mathrm{m})^{-1}$ and $\varepsilon_{\mathrm{r}}=10$. The working frequency is 300 Mhz. Eleven ($N=5$) Fourier harmonics for expanding the contrast along the x-coordinate and $M=6$ step functions of equal width are used for expanding the unknown along the z-axis (fig. 5).

Numerical results concerning the observation domain at height $h=0$ are also given.

These results concern two objects of rectangular section of extent $0.75\,\mathrm{m}\times 1.5\,\mathrm{m}$ whose centers are located at $(-0.75\,\mathrm{m},\ 1.5\,\mathrm{m})$ and $(0.75\,\mathrm{m},\ 1.25\,\mathrm{m})$, respectively, with $\varepsilon=10.1-j0.6$. The domain D has extent $2a=2.5\,\mathrm{m}$ along the x-axis and a depth of $2b=3\,\mathrm{m}$, while the embedding medium has $\sigma_{\mathrm{b}}=10^{-2}\,(\Omega\mathrm{m})^{-1}$ and $\varepsilon_{\mathrm{r}}=10$. The working frequency is 300 Mhz.

The result concerns a more realistic measurement configuration (fig. 6). In particular, a measurement domain with extent equal to 11 m and at $h=0$ is considered and same unknowns as above are searched for. Within this domain we assume 16 uniformly spaced

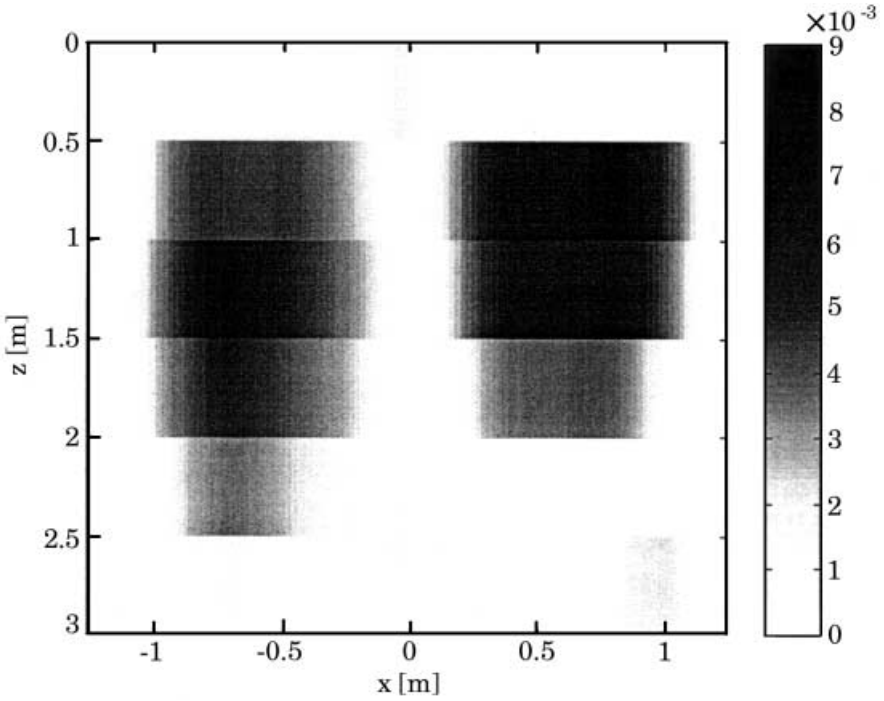

Fig. 5. – Reconstruction by linear inversion of the modulus of the contrast function for two buried objects at frequency of 300 Mhz and with the sources and the receivers at height $h = \lambda$. The data are the samples of the spectrum of the electric scattered field.

locations for the transmitting antenna and 32 equally spaced locations for the receiving antenna.

The numerical results above shown refer to scattered field data obtained thanks to the linear (DBA) model, therefore the necessity of analyzing the stability of the inversion with respect to the model error arises. To this end we now present some results of inversion starting from data obtained by an exact model of the electromagnetic scattering. The result refers to $\varepsilon_r = 15$ and same measurement configuration as the above test case is considered. As one can expect this result is worse than the above one because the model error is larger owing to the increased difference between the dielectric characteristics of the object and the embedding medium (fig. 7).

5. – Conclusions

An analysis of the Distorted Born Approximation (DBA) for the two-dimensional inverse scattering problem of retrieving a buried objects from the knowledge of the scattered field received by filamentary sources located in the free space is given. This analysis makes it possible to investigate the class of the retrievable contrast functions, which exhibit peculiar features as far as their spatial variability is concerned. From the Singular Value Decomposition of the relevant linear operator it has been recognised that the class of the contrast functions which can be reconstructed is defined within a finite-dimensional space, whose features and dimension depend on the reference profile function. In addi-

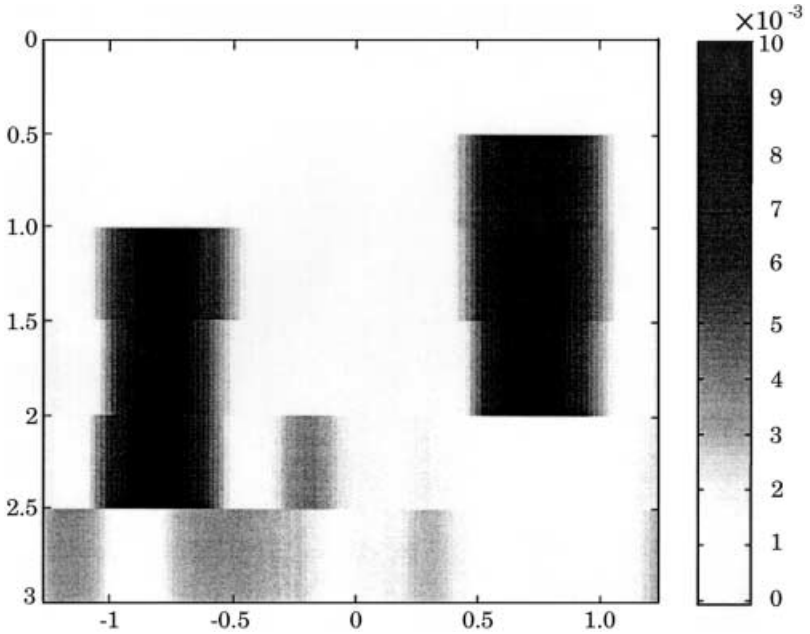

Fig. 6. – Reconstruction by linear inversion of the modulus of the contrast function for two buried objects at frequency of 300 Mhz and with the sources and the receivers at height $h = 0$. The data are collected for 16 equally spaced of the transmitting antenna and at 32 positions of receiving antenna in a domain of 11 m.

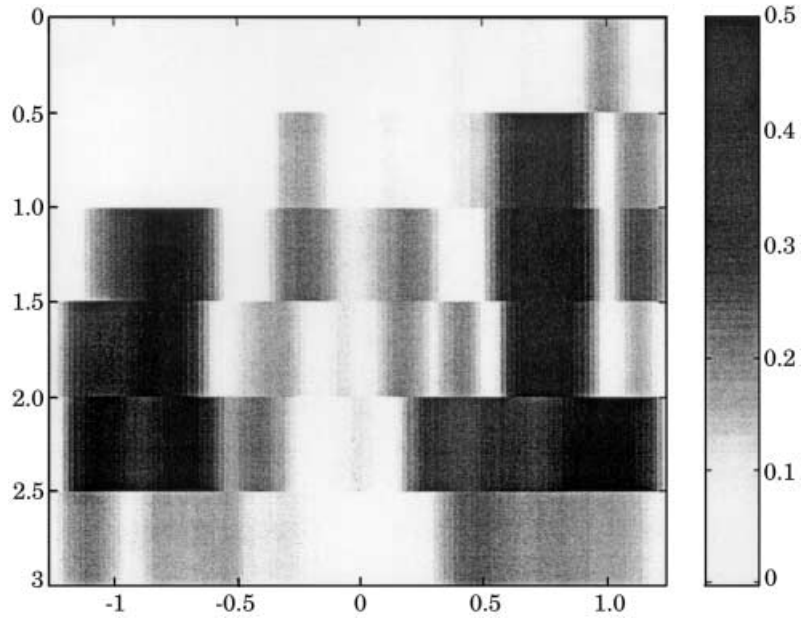

Fig. 7. – Reconstruction by linear inversion of the modulus of the contrast function for two buried objects with $\varepsilon_r = 15$ at frequency of 300 Mhz and with the sources at height $h = 0$. The scattered field is obtained by the exact model of the electromagnetic scattering.

tion, we present an inversion algorithm based on a regularised SVD which makes it possible to face the ill-conditioning problems. Numerical results depicting the effect of the measurement configuration and of error model on the inversions are shown.

The above-performed analysis can be considered preliminary to the investigation of the multifrequency approach, where data are collected at each receiver position at different frequencies, which is of relevant interest in actual set-ups; however, also for this configuration the question of the amount of independent data for optimal frequency sampling is of interest.

In addition, it is also necessary to take into account in the inversion procedure the effect of the radiation pattern of the transmitting and receiving antennas.

The class of the retrievable functions can be enlarged by employing methods based on the inversion of a quadratic operator as it occurred in the Born approximation [18].

Finally, we remark the importance of the analysis performed in this paper also for the problem of determining the shape of buried perfectly conducting objects, where a simplified linear model of the electromagnetic scattering is given under the Kirchoff approximation [19].

* * *

This work was supported by Agenzia Spaziale Italiana.

Appendix

The geometry of the problem is referred in fig. 1. In order to work out the spectral relationship (3) we start with the relationship (2) rewritten with the integration extended to the whole plane instead of the domain D. This is possible because the contrast is equal to zero outside the domain D, as already stressed.

We evaluate the incident field due to a filamentary electrical current located at the abscissa x_s on the line Σ:

$$\mathbf{J} = J\mathbf{i}_y = I_0\delta(x - x_\mathrm{s})\delta(z - h)\mathbf{i}_y. \tag{A.1}$$

The problem is solved by considering the invariance along the y-axis ($\partial/\partial y = 0$) and by introducing the vector potential [20] $\mathbf{A} = A\mathbf{i}_y$, directed along the y-axis. The vector potential satisfies the Helmholtz equation

$$\frac{\partial^2 A}{\partial x^2} + \frac{\partial^2 A}{\partial z^2} + k_i^2 A = -\mu_0 J, \quad i = 0, \mathrm{s}, \tag{A.2}$$

where the subscript i accounts for the fact that the wave number is different in the two half spaces. By substitution of eqs. (A.1) in (A.2) and by performing the Fourier transform with respect to x-variable of both the right- and the left-hand side we obtain

$$-u^2\hat{A} + \frac{\partial^2 \hat{A}}{\partial z^2} + k_i^2\hat{A} = -\mu_0 I_0 \delta(z - h)\exp[jux_\mathrm{s}], \tag{A.3}$$

where $\hat{A}(u, z)$ denotes the Fourier transform of $A(x, z)$ with respect to the x-variable. Equation (A.3) admits harmonic solutions as a linear superposition of $\exp[-jw_i(u)z]$ and

$\exp[jw_i(u)z]$ terms, where

$$w_i(u) = \sqrt{k_i^2 - u^2}, \quad i = 0, \mathrm{s}. \tag{A.4}$$

The coefficients that "weights" the two solutions are different in the three regions $z > 0$, $0 > z > h$, $z < h$, and must be determined by imposing:

1. The continuity of tangential components of the electrical and magnetic field at the interface between the two half-spaces.
2. The continuity of $\hat{A}$ at quote $z = h$.
3. The result of integration of eq. (A.3) between the quotes $z = h^-$ and $z = h^+$.
4. The Sommerfield radiation condition [20].

After calculating $\hat{A}$ the vector potential is retrieved by inverse Fourier transform, and then the incident field is worked out. This provides the following expression of the incident field:

$$E_{\mathrm{inc}}(x,z) = -\frac{\mu_0 \omega I_0}{2\pi} \int_{-\infty}^{+\infty} \frac{\exp[jw_0(u)h]\exp[-jw_{\mathrm{s}}(u)z]}{[w_0(u) + w_{\mathrm{s}}(u)]} \exp[ju(x - x_{\mathrm{s}})]\,\mathrm{d}u. \tag{A.5}$$

Because of the reciprocity theorem, this provides also the external Green's function of the problem as

$$G(x,z,x',z') = -\frac{j}{2\pi} \int_{-\infty}^{+\infty} \frac{\exp[jw_0(u')z]\exp[-jw_{\mathrm{s}}(u')z']}{[w_0(u') + w_{\mathrm{s}}(u')]} \exp[-ju'(x - x')]\,\mathrm{d}u'. \tag{A.6}$$

By (A.5) and (A.6) it steams that the scattered field, as a function of the observation abscissa x and the source abscissa x_{s}, is seen to be equal to the inverse Fourier transform of the second member of eq. (3).

Let us turn now to consider the TE polarization where the incident field is due to a filamentary magnetic current located at the abscissa x_{s} on the line Σ:

$$\mathbf{J}_m = J_m \mathbf{i}_y = \mathbf{I}_{0m} \delta(x - x_{\mathrm{s}}) \delta(z - h) \mathbf{i}_y. \tag{A.7}$$

The problem is solved by introducing the vector potential for the electrical field $\mathbf{A}_m = A_m \mathbf{i}_y$ which is directed along the y-axis and satisfies the following Helmholtz equation:

$$\frac{\partial^2 A_m}{\partial x^2} + \frac{\partial^2 A_m}{\partial z^2} + k_i^2 A_m = -\varepsilon_i J_m, \quad i = 0, \mathrm{s}. \tag{A.8}$$

In a way similar to above from (A.8) the following relationship is obtained:

$$-u^2 \hat{A}_m + \frac{\partial^2 \hat{A}_m}{\partial z^2} + k_i^2 \hat{A}_m = -\varepsilon_i I_{0m} \delta(z - h) \exp[-jux_{\mathrm{s}}], \tag{A.9}$$

where $\hat{A}_m(u,z)$ denotes the Fourier transform of $A_m(x,z)$ with respect to the x-variable.

Equation (A.9) is solved by accounting for the same four above boundary conditions. After calculating $\hat{A}_m$ the incident field is obtained as

$$E_{\mathrm{inc}x}(x,z) = -\frac{I_{0m}}{2\pi}\int_{-\infty}^{+\infty} \frac{w_{\mathrm{s}}(u)\exp[jw_0(u)h]\exp[-jw_{\mathrm{s}}(u)z]}{[\varepsilon_{\mathrm{b}}w_0(u)+w_{\mathrm{s}}(u)]}\exp[ju(x-x_{\mathrm{s}})]\,\mathrm{d}u \tag{A.10}$$

$$E_{\mathrm{inc}z}(x,z) = -\frac{I_{0m}}{2\pi}\int_{-\infty}^{+\infty} \frac{u\exp[jw_0(u)h]\exp[-jw_{\mathrm{s}}(u)z]}{[\varepsilon_{\mathrm{b}}w_0(u)+w_{\mathrm{s}}(u)]}\exp\left[ju(x-x_{\mathrm{s}})\right]\mathrm{d}u. \tag{A.11}$$

In order to calculate the external dyadic Green's function, we have evaluated:

- the x-component of the electrical field in $\mathbf{r}=(x,z)$ (with $z<0$), due to an electrical impulsive source located in $\mathbf{r}'=(x',z')$ (with $x'>0$) and directed along the x-axis,
- the z-component of the electrical field in $\mathbf{r}=(x,z)$ (with $z<0$), due to an electrical impulsive source located in $\mathbf{r}'=(x',z')$ (with $x'>0$) and directed along the x-axis,
- the x-component of the electrical field in $\mathbf{r}=(x,z)$ (with $z<0$), due to an electrical impulsive source located in $\mathbf{r}'=(x',z')$ (with $x'>0$) and directed along the z-axis,
- the z-component of the electrical field in $\mathbf{r}=(x,z)$ (with $z<0$), due to an electrical impulsive source located in $\mathbf{r}'=(x',z')$ (with $x'>0$) and directed along the z-axis.

By definition, these quantities are respectively the four components of the dyadic Green's function $\underline{\mathbf{G}}_{\mathrm{e}}(x,z,x',z')$. The calculations are similar to those exposed for TM polarization and we obtain

$$\underline{\mathbf{G}}_{\mathrm{e}}(x,z,x',z') = \frac{1}{2\pi\omega\varepsilon_0}\int_{-\infty}^{+\infty}\begin{pmatrix} -w_1(u')w_2(u') & w_1(u')u' \\ w_2(u')u' & -(u')^2 \end{pmatrix}\times \tag{A.12}$$

$$\times\,\frac{\exp[jw_1(u')z]\exp[-jw_2(u')z']}{[\varepsilon_{\mathrm{b}}w_1(u')+w_2(u')]}\exp[ju'(x-x')]\,\mathrm{d}u'.$$

Finally, the two components $E_{\mathrm{s}x}$ and $E_{\mathrm{s}z}$ of the scattered field, as a function of x and x_{s}, are equal, respectively, to the inverse Fourier transforms of the second members of eqs. (8) and (9).

REFERENCES

[1] Colton D. and Kress R., *Inverse Acoustic and Electromagnetic Scattering Theory* (Springer Verlag) 1992.
[2] Chew W. C. and Wang Y. M., *IEEE Trans. Medical Imaging.*, **MI-9** (1990) 218.
[3] Chommeloux L., Pichot C. and Bolomey J. C., *IEEE Trans. Microwave Th. Tech.*, **MTT-34** (1986) 1064.
[4] Tabbara W., Duchene B., Pichot C., Lesselier D., Chommeloux L. and Joachimowitz N., *Inverse Problems*, **4** (1988) 305.
[5] Molyneoux J. E. and Witten A., *IEEE Trans. Geosci. Remote Sensing*, **31** (1993) 507.
[6] Deming R. W. and Devaney A. J., *Inverse Problems*, **13** (1997) 29.
[7] Witten A., Won I. J. and Norton S. J., *Inverse Problems*, **13** (1997) 1821.

[8] Bertero M., in *Advances in Electronics and Electron Physics* (Academic Press) 1989, pp. 1-122.
[9] Pierri R. and Soldovieri F., *Inverse Problems*, **14** (1998) 321.
[10] Brancaccio A., Leone G. and Pierri R., *J. Opt. Soc. Am. A*, **15** (1998) 1909.
[11] Leone G., Persico R. and Pierri R., *J. Opt. Soc. Am. A*, **16** (1999) 1779.
[12] Chew W. C., *Waves and Fields in Inhomegeneous Media* (IEEE Press) 1995.
[13] Joachimowitz N., Pichot C. and Hugonin J. P., *IEEE Trans. Antennas Prop.*, **AP-39** (1991) 1742.
[14] Landau H. J. and Pollack H. O., *Bell System Techique J.*, **41** (1962) 1295.
[15] Pierri R., Persico R. and Bernini R., *J. Opt. Soc. Am. A*, **16** (1999) 2392.
[16] Gori F. and Guattari G., *Optics Commun.*, **7** (1973) 163.
[17] Twomey S., *J. Franklin Institute*, **279** (1965) 95.
[18] Pierri R. and Leone G., *IEEE Trans. Geosci. Remote Sensing*, **37** (1999) 374.
[19] Pierri R., Liseno A. and Soldovieri F., *Shape reconstruction from P.O. multifrequency scattered fields via the Singular Value Decomposition approach*, to appear on *IEEE Trans. Antennas Prop., October 2001.*
[20] Kong J. A., *Electromagnetic Wave Theory* (John Wiley and Sons) 1990.